J. Appl. Environ. Biol. Sci., 5(9S)413-427, 2015

ISSN: 2090-4274
Journal of Applied Environmental and Biological Sciences
www.textroad.com

Developing a Numerical and Analytical Model of Fatigue Crack Growth Rate in Rock

A. Refahi[1], M. Abdolmaleki[2], E. Poursaeidi[3]

[1]Assistant Professor, Department of Mining, Faculty of Engineering, University of Zanjan, Zanjan, Iran.
[2]MSc student, Department of Mining, Faculty of Engineering, University of Zanjan, Zanjan, Iran.
[3]Associate Professor, Department of Mechanic, Faculty of Engineering, University of Zanjan, Zanjan, Iran.

Received: March 26, 2015
Accepted: May 17, 2015

ABSTRACT

In this study, fatigue behavior of rock was analytically and numerically modeled. For this purpose, three point of fatigue bending tests were carried out on Limestone specimens prepared from Urmia mine in Iran. Subsequently, the fatigue life and crack growth rate in Limestone were analytically (based on the nonlinear fracture mechanics) and numerically (based on finite element method; FEM) were modeled; the stress intensity factor of FEM models was calculated by J integral and crack tip opening displacement (CTOD). The obtained results showed that although, the analytical approach could fairly predict the fatigue behavior, the fatigue life and crack growth rate evaluated from finite element method had higher agreement with experimental data. In addition, the best results were obtained from FEM models based on J integral method.

KEYWORDS: Fatigue life, Fatigue Crack Growth, Nonlinear Fracture Mechanics, Paris Law, Finite Element Method

1. INTRODUCTION

Fatigue behavior of rocks has been studied by many researches since 1960. Burdin showed that the fatigue strength of a rock depended on its grain size, where fine-grained rocks had the most strength [1]. Haimson and Kim illustrated that increasing strain in rocks under cyclic loading was divided into three sections that were strain growth, a reducing acceleration, a constant acceleration and finally an enhancing acceleration [2]. In addition, Haimson showed that the rate of fatigue crack growth in Granite specimens increased with applying higher stress cycles [3]. After that, in order to determine the effect of loading amplitude on the fatigue life of rocks [4], the fatigue crack growth in brittle sandstones [5], Dynamic Cumulative damage in brittle materials such as rocks [6], nonlinear elastic behavior of sandstone and marble specimens under cyclic loading [7,8], microscopic observation of the fractured granite specimens during compressive fatigue test [9], process of increasing density of small cracks over time and damage of rocks under cyclic loading [10, 11] and effect of cyclic loading on reducing rate of mechanical properties of salt stone [12]. Watanabe and Chen showed the growth rate of cracks in granite specimens respectively occurred in three steps that were growing with a low speed, a constant speed and a high speed [13].

In this study, the fatigue of rock under constant cyclic loading was numerically and analytically modeled. For this purpose, some cubic specimens of Limestone (prepared form Urmia mine in Iran) were made and a static and a fatigue three point bending test were applied; the fatigue life and crack growth rate in specimens were examined. Subsequently, the fatigue behavior of Limestone and crack growth in specimens numerically modeled using finite element method and it was analytically modeled using based on nonlinear fracture mechanics. In order to validate the obtained results, they were compared by experimentally evaluated data.

2. MATERIALS AND METHODS

In this study, to verify the obtained results from modeling, they were compared by the experimentally evaluated data from applying standard tests to Limestone specimens prepared from Urmia Mine in Iran. To estimate the mechanical properties of Limestone, a standard uniaxial compressive test was carried out on ten cylindrical specimens of Limestone with 110 mm height and 54 mm diameter as shown in Fig.1a. In order to determine elastic modulus and Poisson's ratio of the specimens, three strain gages were used. In addition, ten cubic specimens with 5*5*20 cm dimensions of Limestone were prepared as shown in Fig. 1b, and then a standard three point bending test was applied to them using an Instron universal testing machine (Fig. 2). The specimens were located on two-roller supports with 12 cm apart and the force was applied by a rigid cylinder with 10 mm in diameter acting on the middle part of the specimen under the displacement rate of 0.5 mm/min until the first crack appears in the concretes. To obtain the accurate results, the surface of the specimens was

Corresponding Author: A. Refahi, Assistant Professor, Department of Mining, Faculty of Engineering, University of Zanjan, Zanjan, Iran. E-mail: refahi.arash@znu.ac.it; refahi.arash@gmail.com Tel: +989123034360

constantly monitored during the experiment by stopping the test and accurate examination using dye penetrate technique.

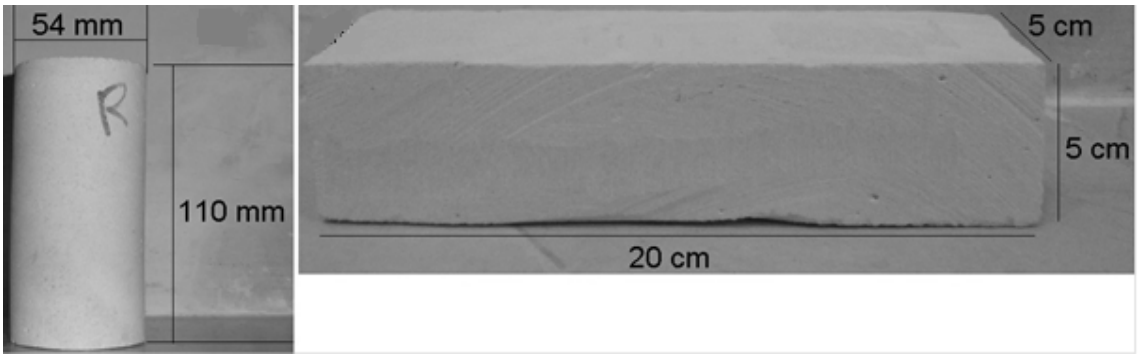

Fig. 1. Cylindrical and cubic specimen of Limestone.

In order to determine the fatigue life of rock under constant cyclic loading, a standard fatigue bending test was carried out on ten specimens of Limestone using Instron universal testing Machine; the dimensions of the fatigue specimens was similar to that of the three point bending test. The frequency of cyclic loading was 1 Hz in the sinusoidal waveform. The maximum applied load was 70%, 80% and 90% of the fracture load in the static bending test (0.7, 0.8 and 0.9*F_{max}). In order to obtain the rate of fatigue crack growth, the generated crack after applying static-bending load was taken as the initial crack length. The minimum load was zero. The crack lengths during growth were examined using a special designed microscope.

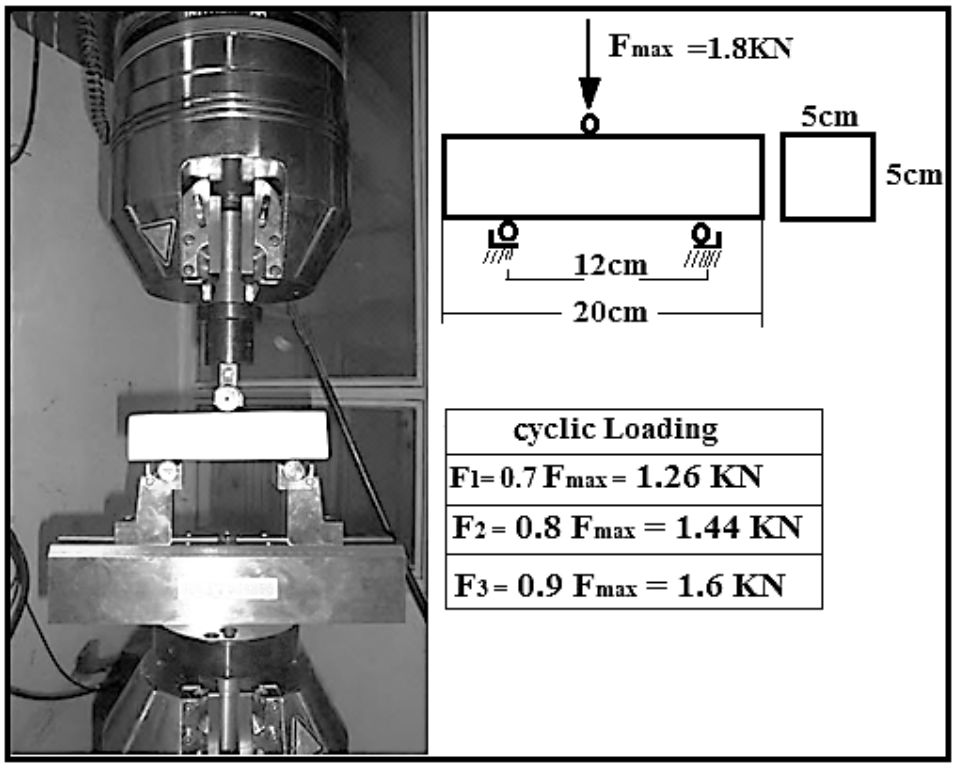

Fig. 2. Instron universal testing machine.

3. RESULTS AND DISCUSSION

The scatter of experimentally obtained results was remarkably high. This is common for rocks under loading where the flaws vary in size, shape and orientation, causing the strength of rocks to vary from specimen to specimen [14]. Weibull statistical approach was used to determine the statistically most probable result. The basic assumption in Weibull distribution is that a body of materials has a statistical distribution of noninteracting

fractures. If there are N broken specimens of a brittle material that were tested, the fracture probability of ith specimen ($F_i(V)$) is equal to:

$$F_i(V) = \frac{i}{N+1} \quad (1)$$

Based on Weibull distribution, the fracture probability of each specimen can be related to the applied stress (σ) as follows:

$$1 - F(V) = \exp\left[\left(\frac{\sigma}{\sigma_0}\right)^m\right] \quad (2)$$

Where σ_0 is a characteristic strength of the materials that it is often defined as the mean strength of material, and m is the Weibull modulus measuring the variability of strength of materials; the higher the value of m, the less is the materials variability in strength. A double-logarithmic plot of Eq. (2) will give a straight line with slope m expressed as follows [14]:

$$\ln\left[\ln\left(\frac{1}{1-F(V)}\right)\right] = m\ln\sigma - m\ln\sigma_0 \quad (3)$$

Consequently, by formatting Eq. (3) for the compressive strength, bending fracture load, elastic modulus and Poisson's ratio, and then by passing the best line through the experimental data using the regression approach, the mean value of mechanical properties of Limestone was determined and presented in Table 1 [15]. Similar to the static test, the mean value of fatigue life, initial crack length and final crack length prior to fracture of Limestone was determined and presented in Table 2. Furthermore, the crack growth rate during the fatigue test is shown in Fig. 3. The obtained results showed that the ultimate crack length prior to final fracture and fatigue life of the rock specimens decreased by increasing the applied maximum load during the test.

Table 1. Mean value of mechanical properties of Urmia Limestone.

Mechanical properties	Mean uniaxial compressive strength MPa	Mean elastic modulus GPa	Mean Poisson's ratio	Mean bending fracture load KN
Limestone	118.37	27	0.2	1.78

Table 2. Mean value of results obtained from fatigue test.

Maximum applied load KN	Mean length of initial crack mm	Mean length of final crack mm	Mean fatigue life
1.26	6.5	42.75	1185
1.44	9.5	33.75	490
1.6	13.5	31.5	135

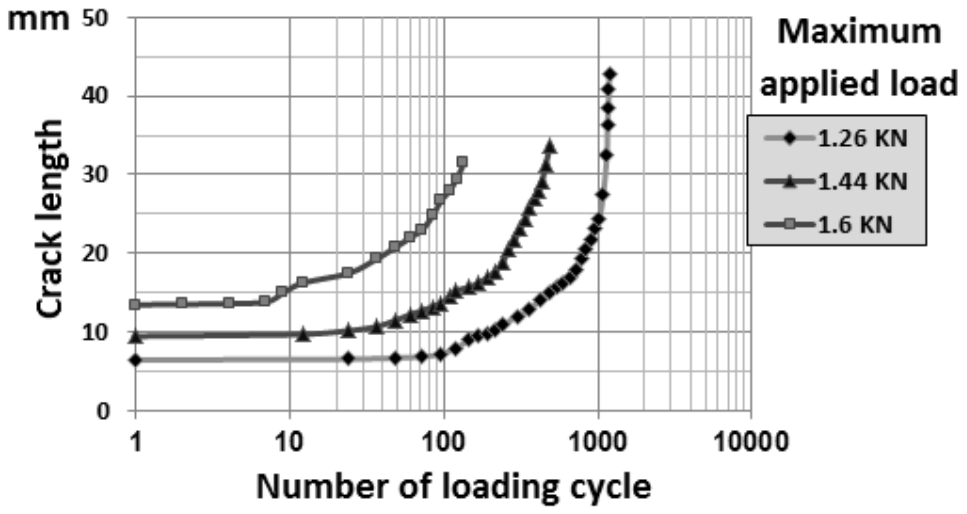

Fig. 3. Growth of fatigue crack length in Limestone specimens.

4. Analytically Measuring Fatigue Life of rock

In order to investigate the fatigue behavior of quasi-brittle materials such as rock and concrete, non-linear elastic fracture mechanics was used because of the large size of the plastic zone at the tip of the crack. Many researchers studied the size effect of samples and tried to use from non-linear elastic fracture mechanics (NLFM) and the Paris law for calculating the fatigue behavior. In this study, the fatigue method based on the failure of the two-dimensional Subramaniam et al [16-19] was used.

Based on this method, the speed of crack growth decreases before crack length reaches the critical value (a_c), subsequently, the speed will increase (Fig. 4). Thus, the propagation of crack length (Δa) can be divided into two stages: deceleration stage and acceleration stage. Subramaniam et al. [19] concluded that the deceleration stage could be described by the following equation:

$$\frac{\Delta a}{\Delta N} = C_1 (a - a_0)^{n_1} \qquad \text{for} \quad a < a_c \tag{4}$$

Where a and a_0 are current crack length and initial crack length, respectively. C_1 and n_1 are calibration constants depending on structural geometry, boundary conditions and type of materials and ΔN is increment of loading cycles.

The critical crack length (a_c), which is defined by the inflection point of the crack length-number of loading cycles curve (Fig. 4a), is almost equal to the crack length at the peak monotonic load level [19]. The crack growth characteristics in the acceleration stage are governed by the change in stress intensity factor (ΔK) during each load cycle based on Paris Law [20, 21]:

$$\frac{\Delta a}{\Delta N} = C_2 (\Delta K)^{n_2} \qquad \text{for} \quad a > a_c \tag{5}$$

Where ΔK_I is the mode I stress intensity factor in each cycle ($\mathrm{MPa}\sqrt{\mathrm{mm}}$). C_2 and n_2 are calibration constants related to the structural geometry, boundary conditions, and material type. In addition, stress intensity factor (K_I) can be calculated using following equations [22]:

$$K_I = \frac{PS}{BW^{\frac{2}{3}}} f(\frac{a}{W})$$

$$f(\frac{a}{W}) = \frac{3(\frac{a}{W})^{\frac{1}{2}} \left[1.99 - \frac{a}{W}\left(1 - \frac{a}{W}\right)\left(2.15 - 3.93(\frac{a}{W}) + 2.7(\frac{a}{W})^2\right)\right]}{2\left[1 + 2(\frac{a}{W})\right]\left[1 - (\frac{a}{W})\right]^{\frac{3}{2}}} \tag{6}$$

Where a is the crack length, S is the distance between the fulcrums, W and B are the width and thickness of the sample, respectively, and P is the applied load.

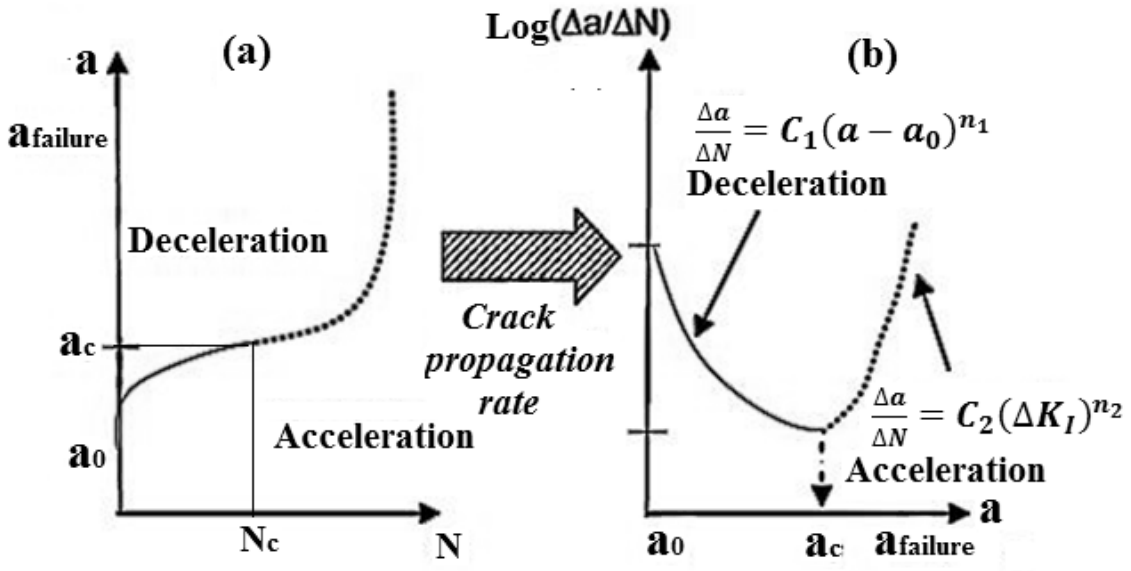

Fig. 4. (a) Increasing crack length versus number of cycles, and (b), the crack growth rate changes during increasing crack length [19].

In order to calculate the critical crack length (a_c)equal to the turning point of loading cycles-crack length curve, the best line passing through the experimentally obtained data using the regression approach was determined (Fig. 4) and then a_c was calculated (Table 3). Fig. 5 shows the logarithmic curve of crack growth rate (da/dN) versus the crack growth (da) before the crack length reaches the critical value. C_1 and n_1 could be evaluated by passing the best line among the data presented in Fig. 5 (based on Eq. (4)); the obtained results were shown in Table 3. Subsequently, by rewriting Eq. (4) and solving the following integral, the number of loading cycles until the critical crack length was calculated (Table 3) [19].

$$N_{dec} = \int_{a_0}^{a_c} \frac{da}{C_1(a - a_0)^{n_1}} \quad (7)$$

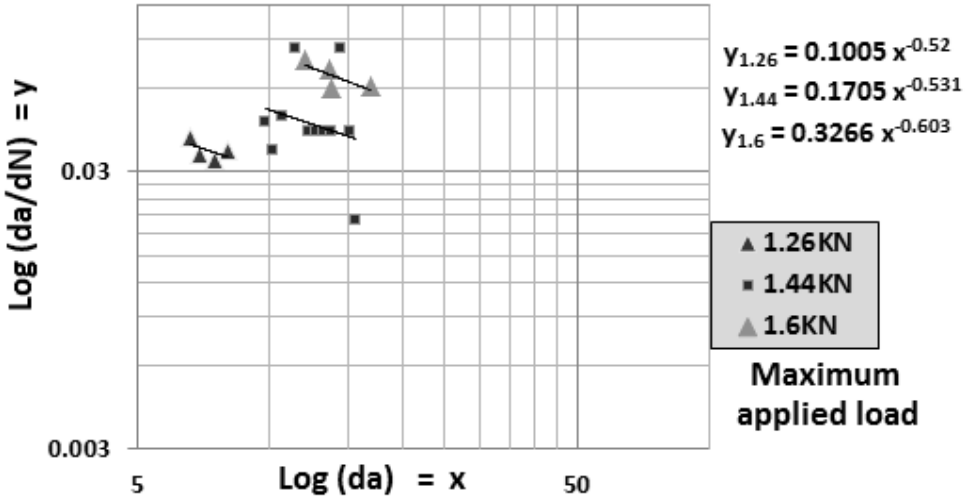

Fig. 5. Logarithmic curve of crack growth rate versus crack length before the crack length reaches the critical value (da is given in mm).

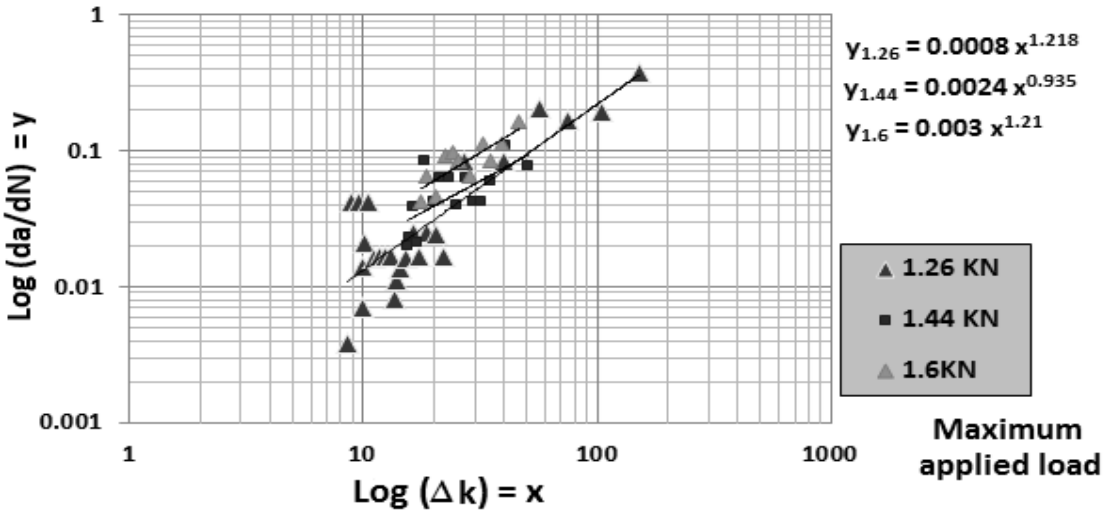

Fig. 6. Logarithmic curve of crack growth rate versus mode I stress intensity factor after the crack length reaches the critical value (da and k is given in mm and $MPa\sqrt{m}$ respectively).

In order to evaluate the number of loading cycles until fracture when the crack length is larger than the critical value, the stress intensity factor was first calculated using Eq. (6) in each loading cycle, and then the logarithmic graph of the stress intensity-crack growth rate was determined as shown in Fig. 6. By passage of a best line among the obtained results (Fig .6) using regression approach, C_2 and n_2 could be evaluated based on Eq. (5) as presented in Table 3. Subsequently, by rewriting Eq. (5) for acceleration stage ($a > a_c$) and solving the following integral, the number of loading cycles until fracture was calculated (Table 3) [20, 21].

$$N_{acc} = \int_{a_c}^{a_f} \frac{da}{C_2 (\Delta K)^{n_2}} \qquad (8)$$

Where a_f is the mean final crack length prior fracture. As shown in Table 3, there is fairly good agreement between analytically calculated fatigue life and those experimentally evaluated; at the low cyclic loading, this method is more efficient. The error of predicting fatigue life in the acceleration stage of crack growth rate (N_{acc}) is lower than that in the deceleration stage. However, all experimental fatigue lives in the deceleration stage (N_{dec}) are less than those in acceleration stage.

Table 3. Results obtained from analytically modeling fatigue crack growth rate.

Applied maximum load (KN)	Critical crack length (mm)	Material constants				Fatigue life (cycle)			Prediction Error (%)		
		C_1	n_1	C_2	n_2	Analytical N_{dec}	Analytical N_{acc}	Exp. Result	N_{dec}	N_{acc}	N_{tot}
1.26	7.25	0.1005	-0.52	0.0008	1.218	84	1114	1185	-12.5	2.3	1.09
1.44	15.75	0.1705	-0.531	0.0024	0.935	135	369	490	-6.9	6.95	2.86
1.6	15	0.3	-0.6	0.003	1.2	12	107	135	22.2	17.75	11.85

5. Numerical Fatigue Crack Growth Modeling

In this study, fatigue crack growth has been simulated using ABAQUS and ZENCRACK software based on finite element method (FEM) in three dimensions; with ZENCRACK, in order to analyze fatigue cracks numerically, fracture mechanics parameters (stress intensity factor, K_I and energy release rate, G) were obtained based on CTOD and Energy methods [23]. The theory of crack tip opening displacement (CTOD) and J integral (energy method) were used as described in appendix A [23]. In order to stimulate three-dimensional fatigue crack growth numerically, first, uncrack mesh model was generated. For this purpose, the geometry of the specimens (Regardless crack) and the bending test conditions were modeled in the finite element software ABAQUS; the hexahedron brick elements of quadratic twenty-node (C3D20R) were used (Fig.7). Then, the uncrack mesh model was introduced to ZENCRACK and a primary crack with length presented in Table 2 was generated in the middle of specimen through replacing a series of meshed crack blocks called s03_t23x1 (Fig. 8).

Then, according to the use of Paris law [20,21], through combining data from the three loading levels related to acceleration stage (Fig. 6) in a graph (fig. 9), and passing an exponential regression line from the graph points, the final calibration constants for use in the software, namely, c_2 and n_2, were obtained 0.0008 and 1.2714 respectively. Subsequently, fatigue tests were carried out by defining the material final constants and fracture toughness (critical stress intensity factor, K_c) presented in Table 4 and the stress intensity factor calculated using the CTOD and J integral method. Finally, the fatigue life of specimen was calculated using Paris law [20, 21]. Fig. 10 shows the crack growth fatigue in the finite element model of Limestone under 1.6KN maximum applied load.

The obtained fatigue life of Limestone was presented in Table 4, and the determined growth of crack length was shown in Fig. 11; it seems that the finite element method is able to predict the fatigue behavior of Limestone specimens well. The crack growth versus the calculated stress intensity factors is shown in Fig. 12-14. It seems that the agreement between numerically analyzed results of fatigue crack growth and the experimental data are more than this agreement for the analytical results. In addition, it is clear that the numerical results obtained based on J integral method are closer to the experimental results than those obtained based on CTOD method.

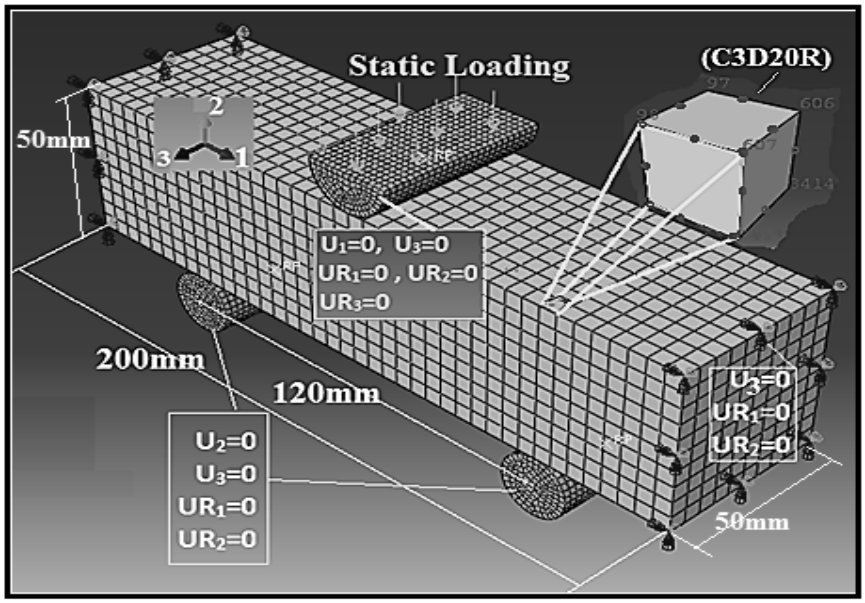

Fig 7. Finite element model of static-bending test applied on cubic limestone in ABAQUS software (U and UR are components of displacement).

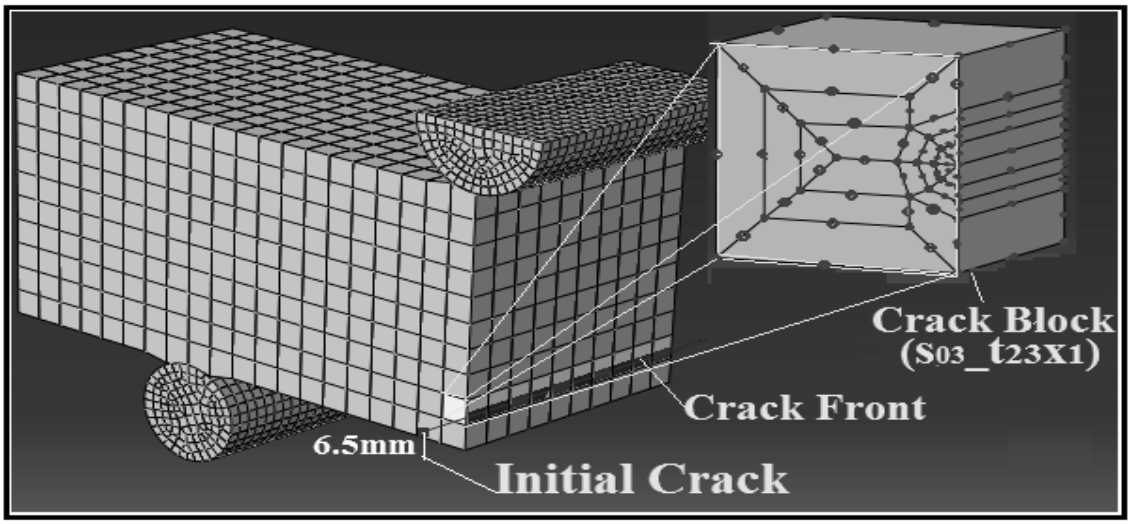

Fig. 8. Finite element model of fatigue bending test applied on cubic limestone including an initial crack in ZENCRACK software.

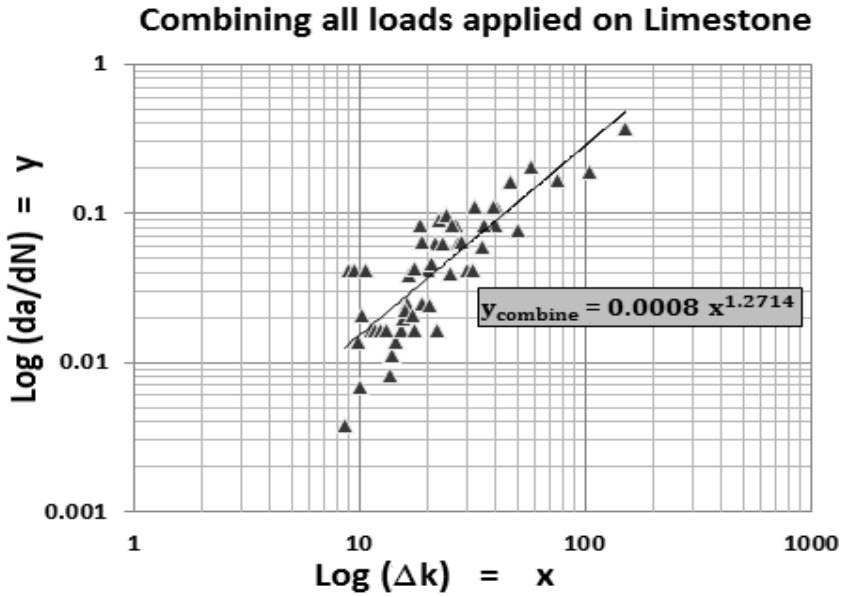

Fig 9. The combination of experimental data related to acceleration stage (crack growth rate - stress intensity factors) to determine the calibration constants used in the numerical method (da and k is given in mm and $MPa\sqrt{m}$ respectively).

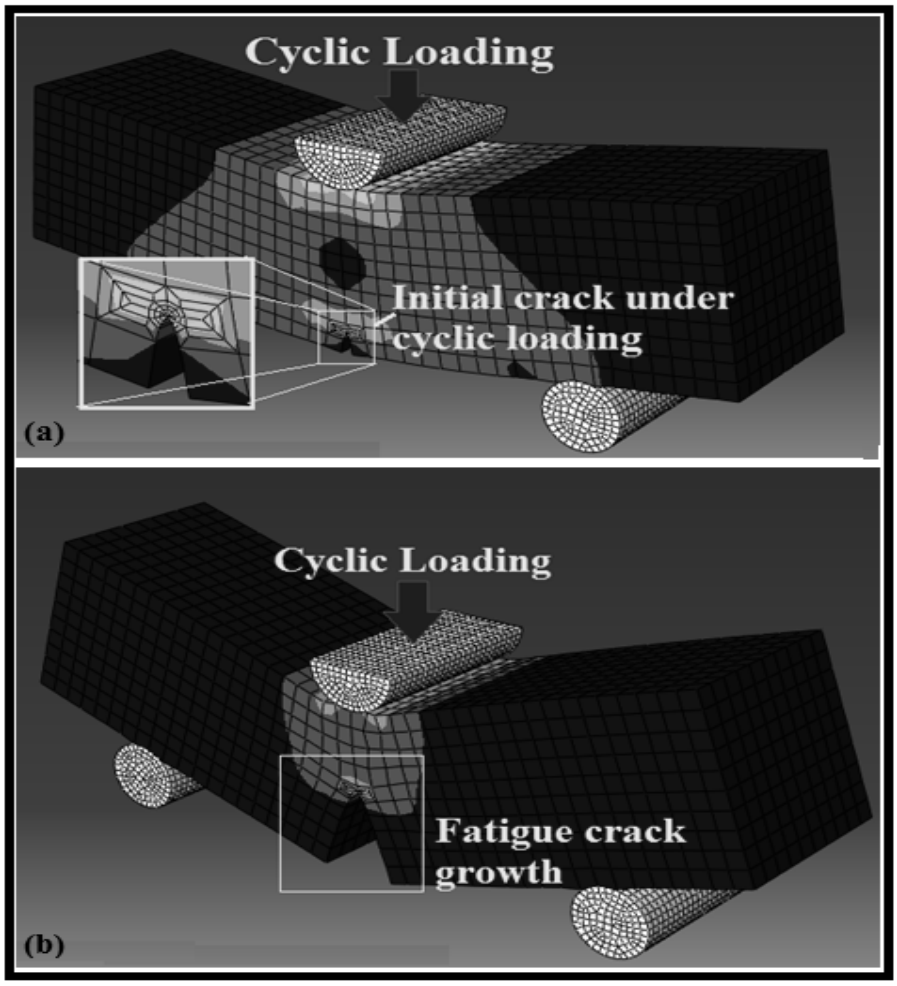

Fig. 10. Finite element analysis of fatigue crack growth.

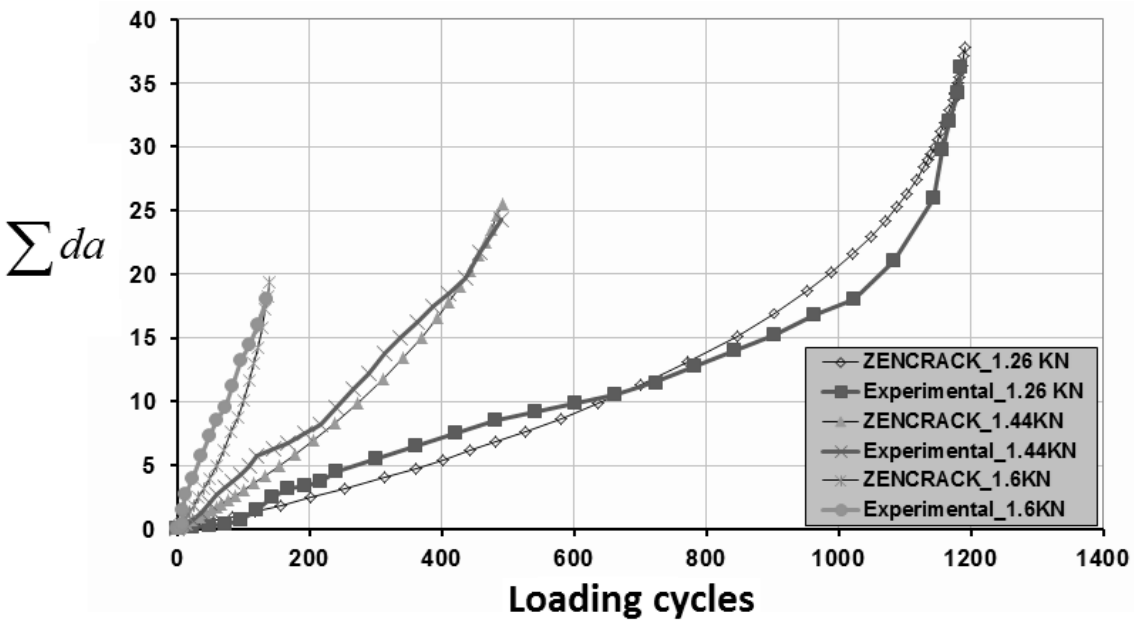

Fig 11. Crack length versus cycle number, from the numerical simulation and experimental results for constant amplitude cyclic loading with load values 1.26, 1.44 and 1.6 KN (da is given in mm).

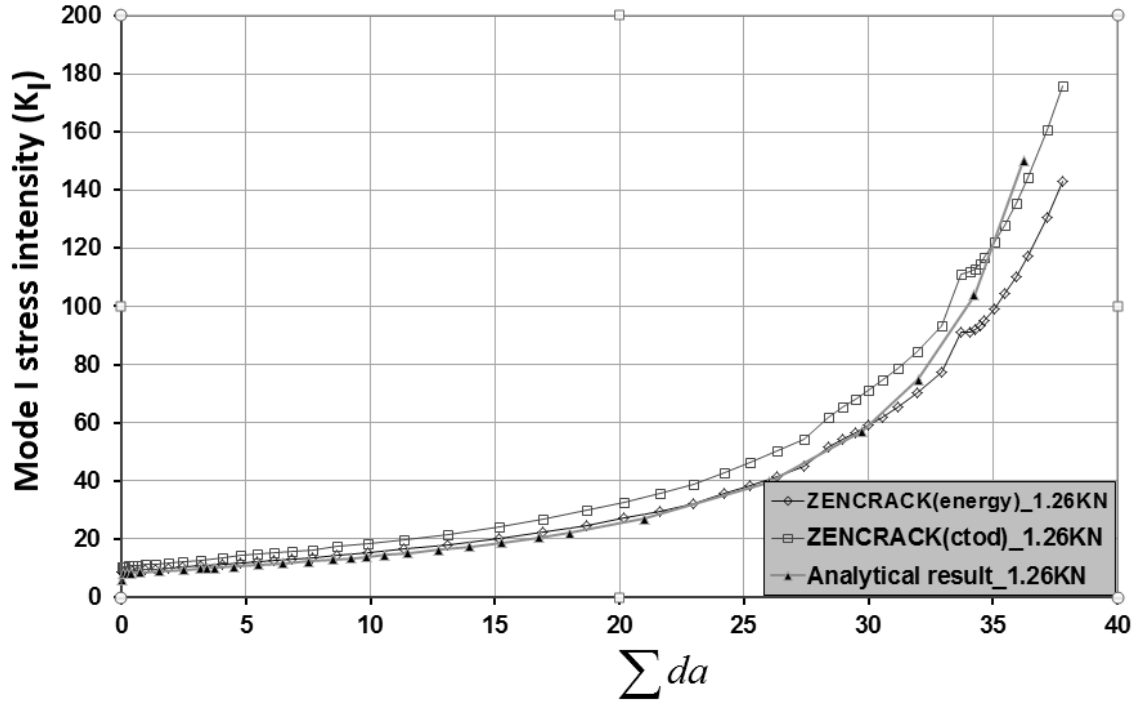

Fig. 12. Crack length stress intensity factor, from the numerical simulation and experimental results for constant amplitude cyclic loading with load value1.26 KN (da and k is given in mm and $MPa\sqrt{m}$ respectively).

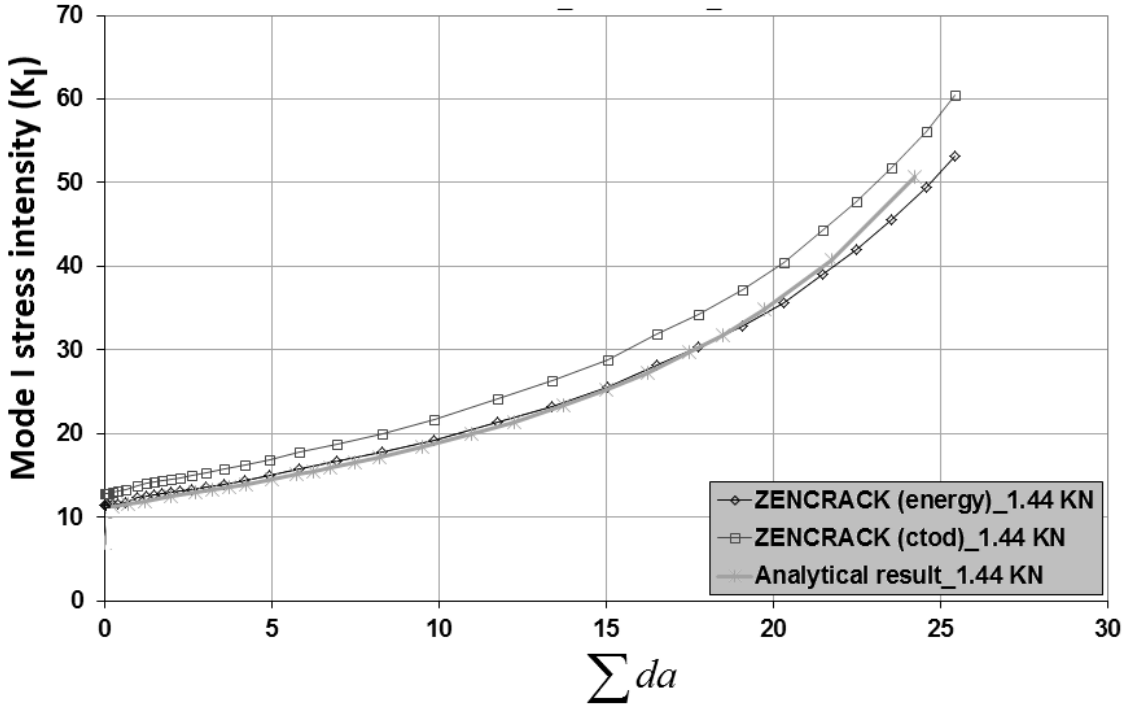

Fig 13: The graphs of crack length stress intensity factor, from the numerical simulation and experimental results for constant amplitude cyclic loading with load value1.44 KN

(da and k is given in mm and $MPa\sqrt{m}$ respectively).

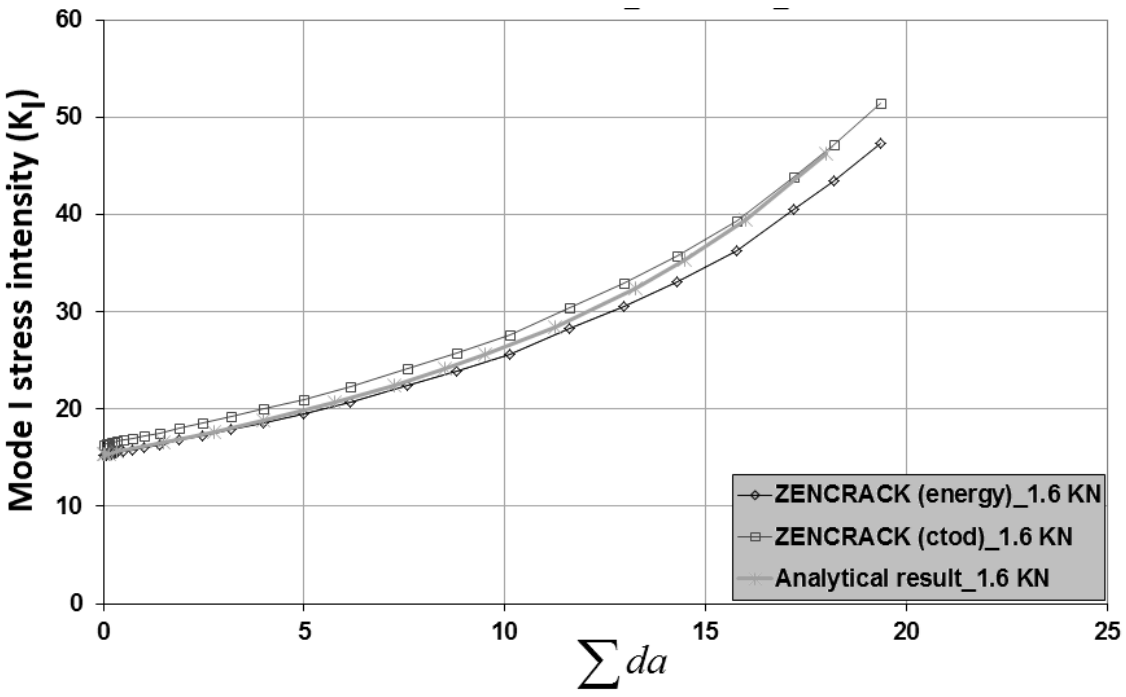

Fig 14: The graphs of crack length stress intensity factor, from the numerical simulation and experimental results for constant amplitude cyclic loading with load value1.6 KN

(da and k is given in mm and $MPa\sqrt{m}$ respectively).

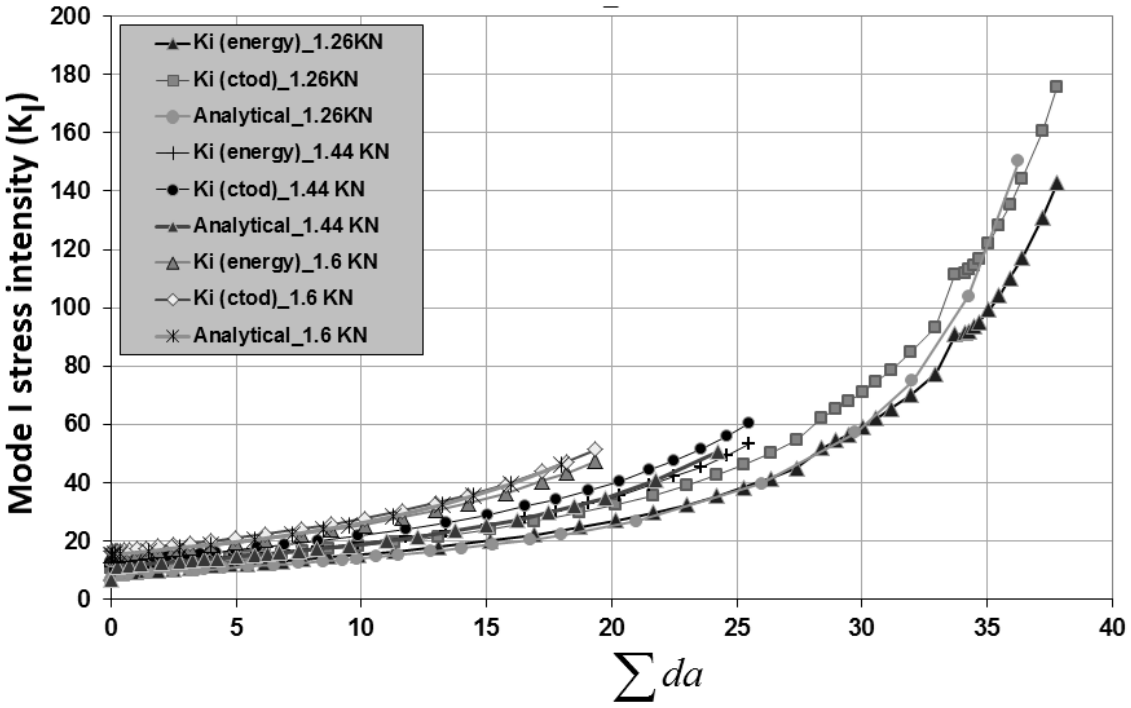

Fig. 15: The curve of crack length-stress intensity factor obtained from the numerical simulation and experimental results for constant amplitude cyclic loading with load values 1.26, 1.44 and 1.6 KN (da and k is given in mm and $MPa\sqrt{m}$ respectively).

Table 4: Fracture toughness and calibration constants and fatigue life prediction by analytical and numerical methods.

Applied maximum load (KN)	Fracture toughness (K_C) $(MPa\sqrt{mm})$			Material constants		Fatigue life (cycle)			Prediction Error (%)	
	$Exp.$	$CTOD$	J_int	C_2	n_2	$N_{\exp}$	N_{anal}	N_{num}	N_{anal}	N_{num}
1.26	150.26	176	143	0.0008	1.2714	1185	1026	1191	-13.41	+0.506
1.44	50.65	60.5	53.1	0.0008	1.2714	490	519	491	+5.92	+0.204
1.6	46.17	51.4	47.3	0.0008	1.2714	135	154	139	+14.07	+2.96

6. Conclusion

In order to examine the fatigue behavior of rock, a three-point bending fatigue test was carried out on cubic specimens of Limestone; the maximum applied load was 70%, 80% and 90% of the fracture load in the static bending test. In addition, fatigue life of Limestone and the growth of crack length during the test were analytically and numerically modeled based on J integral method, CTOD method and the finite element method.

In the analytical method, fatigue life by a combination of basics NLFM and Paris law was predicted. Furthermore, in numerical method, fracture mechanics parameters using the CTOD and Energy methods, were obtained, and a numerical modeling of fatigue crack was performed for both methods. Finally, using Paris law, the fatigue life of specimens, and fatigue crack growth were simulated in three-dimensions.

Based on the obtained results, the following conclusions have been drawn:

- The crack growth rate decreased before that this length reached the critical value, and then it increased until fracture. In addition, by increasing the applied maximum load, the ultimate crack length prior to final fracture and fatigue life decreased.
- Analytically obtained results illustrated that this method could fairly predict the fatigue life of Limestone with the error from 5.92% to 14.07%, but the fatigue life and crack growth rate evaluated from finite element method had higher agreement with the experimental data (i.e. fatigue life error from 0.5% to 2.96%) than the analytical results. Finally, the obtained fatigue life and crack growth rate based on J integral had the highest agreement with the experimental data.

– Above-mentioned analytical and numerical methods, both are successful in predicting the fatigue crack life, with this difference that the analytical method, the calibration constants are much needed, and for low loading levels is highly recommended, however, numerical analysis requires less calibration constants, and can be used for all load levels. Consequently, finite element simulation based on the energy method is the best approach for predicting fatigue behavior of the rock.

Appendix A

A.1. Crack Tip Opening Displacement (CTOD)

This method is an indicator for determining plastic strain. If the CTOD exceeds a critical value, failure occurs. This criterion was first proposed by WELLS [24, 25] and it can analyze crack growth and size of crack tip in plastic zone (Fig. A.1.1). If it is assumed that there is a central crack with 2a length, COD value is [26, 27]:

$$\mathrm{COD} = 2\mathrm{V} = 4\frac{\sigma}{\mathrm{E}} * \sqrt{(\mathrm{a} + \mathrm{rp}\ )^2 - x^2} \qquad \text{(A.1.1)}$$

With replacing $\mathrm{x} = \mathrm{a}$ and regardless from rp square, in the above equation, CTOD value is:

$$CTOD = 4\frac{\sigma}{\mathrm{E}} * \sqrt{2\mathrm{a} * \mathrm{rp}} \qquad \text{(A.1.2)}$$

Where σ and E are stress and elasticity modulus.

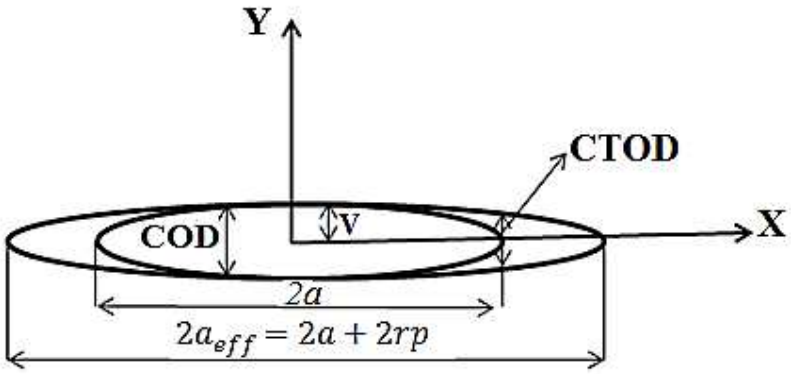

Fig. A.1.1. Opening displacement of a crack [26, 27].

In ZENCRACK, to calculate the stress intensity factor using CTOD method, by defining a local coordinate system at any point of the crack front (Fig. A.1.2), the relative opening displacement of this point is calculated using equation A.1.2, and then the mode I stress intensity factors are calculated considering the obtained displacement by following equation [23]:

$$K_I = \frac{E * V_i}{8B}\sqrt{\frac{2\pi}{r}} \qquad \text{(A.1.3)}$$

$$B = 1 - \upsilon^2 \quad \text{Plane strain}$$

$$B = 1 \quad \text{Plane stress}$$

Where υ is the Poisson's ratio and V_i is the relative displacement of the crack (CTOD). By equation A.1.3, the stress intensity factors can be obtained, and with values stress intensity factors, equivalent energy release rate from the following equation is obtained [23]:

$$G_{eq} = \frac{B}{E} * (K_I^2 + K_{II}^2) + \frac{1}{2G} K_{III}^2$$

$$B = 1 - \upsilon^2 \qquad \text{Plane strain} \qquad \text{(A.1.4)}$$

$$B = 1 \qquad \text{Plane stress}$$

Finally, using stress intensity factors and equivalent energy release rate, fatigue life can be predicted as follows [23]:

$$\frac{da}{dN} = C(\Delta K)^n = C(\Delta\sqrt{G}) \qquad \text{(A.1.5)}$$

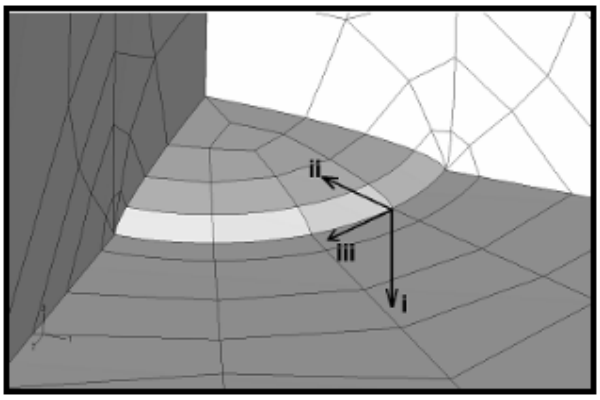

Fig. A.1.2. A local coordinate system defined at each point of the crack length to calculate the displacement in the direction I (opening mode), II (sliding mode) and III (tearing mode) [23].

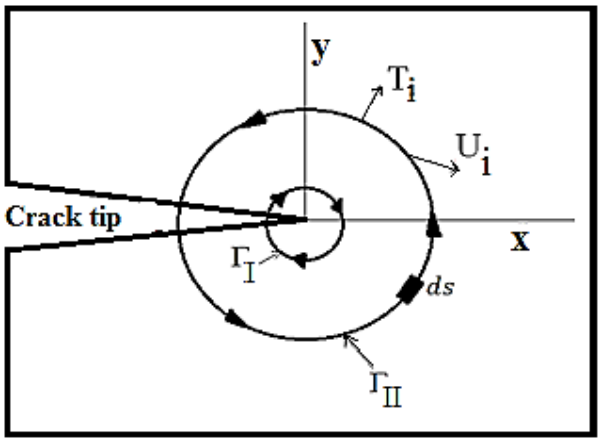

Fig. A.2.1. Selecting the closed contour Γ around the body under stress [28].

A.2. J Integral (Energy Method)

J integral or energy method is applied to determine the fracture behavior of nonlinear materials. J Integral is defined by following equation [28]:

$$J = \int_\Gamma W dy - T \frac{\delta u}{\delta x} dS \qquad \text{(A.2.1)}$$

As shown in Figure A.2.1, Γ is a closed contour in the opposite direction of clockwise, and it surrounds an area of a body under stress. W is elastic energy, T is the stress vector perpendicular to Γ, u is the components of displacement vector in x direction and dS is a longitudinal element of the contour Γ.

Since the J integral is independent of any path, it is easy to calculate the integral. Thus, J-Integral is a simple way to calculate the energy release rate in cases where a large plastic zone exists at crack tip [29]. In the ZENCRACK software, the stress intensity factor at any point in along the crack front can be calculated using J

integral method. Values of J-Integral can be defined as the rate of energy release during crack growth. Assuming a virtual crack growth $\lambda(S)$ in plate of three-dimensional crack growth, J-Integral values can be defined by [30]:

$$G = \int_A n.H.qda \qquad \text{(A.2.2)}$$

Where G is Energy release rate, da is a surface element near the crack tip, n is normal vector of the surface element (da), q is local orientation vector for the virtual crack growth and H is a matrix, which is defined as follows:

$$H = (WI - \sigma \frac{\delta u}{\delta x}) \qquad \text{(A.2.3)}$$

Where W, I, σ and $\delta u/\delta x$ are the elastic energy of materials with elastic behavior, the unit matrix, stress matrix and strain matrix, respectively. Finally with the values of G and use Equations A.1.4, the stress intensity factors can be calculated.

REFERENCES

[1] Burdine, N.T., 1963. Rock failure under dynamic loading conditions. Society of Petroleum Engineers Journal 1–8 March 1963.

[2] Haimson, B.C., Kim, C.M., 1972. Mechanical Behavior of Rock under Cyclic Fatigue. Proceedings of thirteenth Symposium on Rock Mechanics, Illinois, USA, pp. 845–863.

[3] Haimson, B.C., 1978. Effect of cyclic loading on rock. Dynamic Geotechnical Testing, ASTM STP654, Philadelphia, USA, pp. 228–245.

[4] Singh SK. Fatigue and strain hardening behavior of Greywacke from the Flagstaff formation, New South Wales. Engineering Geology 1989; 26:171–9.

[5] Li G, Moelle KH, Lewis JA. Fatigue crack growth in brittle Sandstones. Int. J Rock Mech. Min Sci. Geomech Abstr 1992; 29(5):469–77.

[6] Chen EP. Non local effects on dynamic damage accumulation in brittle solids. Int. J Numer. Anal Mech. Geomech. 1999;23:1–21

[7] Xi DY, Chen YP, Tao YZ. Nonlinear elastic hysteric characteristics of rocks. Chin J Rock Mech. Eng. 2006; 25(6):1086–93.

[8] Xi DY, Chen YP, Tao YZ. Nonlinear elastic hysteric characteristics of rocks. Chin J Rock Mech. Eng. 2006; 25(6):1086–93.

[9] Akesson, U., Hansson, J., Stigh, J., 2004. Characterization of micro cracks in the Bohus granite, western Sweden, caused by uniaxial cyclic loading. Engineering Geology 72, 131–142.

[10] Faulkner, D.R., Mitchell, T.M., Healy, D., Heap, M.J., 2006. Slip on 'weak' faults by the rotation of regional stress in the fracture damage zone. Nature 444, 922–925.

[11] Xiao, J.Q., Ding, D.X. Fatigue damage variable and evolution of rock subjected to cyclic loading Int. J Rock Mech. Min Sci. 20010; 47: 461-468.

[12] Fuenkajorn, K., Phueakphum, D. Effects of cyclic loading on mechanical properties of Maha Sarakham salt. Eng. Geol. 2010; 112:43-52.

[13] Chen,Y., Watanabe, K. Crack growth in Westerly granite during a cyclic loading test. Journal of Engineering Geology 2010; 117: 189–197.

[14] M.A. Meyers, K.K. Chawla, Mechanical behavior of materials, second ed. Cambridge University Press, New York, 2009.

[15] E. Kreyszig, Advanced engineering mathematics, ninth ed. John Wiley & Sons, Singapore, 2006.

[16] Subramaniam KV, Popovics JS, Shah SP. Monitoring fatigue damage in concrete. In: Proceedings MRS fall meeting, vol. 503; 1997. p. 151–7.

[17] Subramaniam KV, Popovics JS, Shah SP. Testing concrete in torsion: instability analysis and experiments. J Eng. Mech., Am Soc. Civil Eng. (ASCE) 1998;124(11):1258–68.

[18] Subramaniam KV, Popovics JS, Shah SP. Fatigue behavior of concrete subjected to biaxial stresses in the C–T Region. Mater J Am Concr Inst. (ACI) 1999;96(6):663–9.
[19] Subramaniam KV, O'Neil E, Popovics JS, Shah SP. Flexural fatigue of concrete: experiments and theoretical model. J Eng. Mech., Am Soc. Civil Eng. (ASCE) 2000; 126(9):891–8.
[20] Paris PC. The growth of fatigue cracks due to variation in load. Ph.D. Thesis, Lehigh University, Bethlehem, PA; 1962.
[21] Paris P, Erdogan F. A critical analysis of crack propagation laws. J Basic Eng., Trans Am Soc. Mech. Eng. 1963(December):528–34.
[22] "Standard Test Method for Measurement of Fracture Toughness" ASTM Designation E1820, Vol. 03.01, ASTM, West Conshohocken, PA 19428-2959.
[23] ZENCRACK background and theory manual, Issue 6, Zentech Inc. 2011.
[24] Wells, A. A., Unstable crack propagation in metals-cleavage and fast fracture, Proc. Crack propagation Symposium, Cranfield (1961) pp.2010-230.
[25] Wells, A. A., Application of fracture mechanics at and beyond general yielding, British Welding Research Ass. Rep. M13,(1963).
[26] Meguid S.A., "Engineering Fracture Mechanics", Elsevier Applied Science Publishers, England, June 1989.
[27] Shah S.P & Swarts S.E. & ouyang C., "Fracture Mechanics of Concrete: Application of fracture Mechanics to Concrete, Rock and Other Quasi-Brittle Materials", John Wiely and Sonc Inc., 1995.
[28] Broek D. Elementary engineering fracture mechanics. The Hague: Martinus Nijhoff Publishers, 1986.
[29] Rice, J.R., A path independent integral and approximate analysis of strain concentrations by notches cracks, J. Appl. Mech. (1968) pp. 379-386.
[30] Abaqus Analysis user's manual, Dassault Inc. 2010.